

Spectrum of Doubly Ionized Xenon (Xe III)

W. Persson and C.-G. Wahlström

Department of Physics, Lund Institute of Technology, Box 118, S-221 00 Lund, Sweden

G. Bertuccelli and H. O. Di Rocco

Departamento de Física, Facultad de Ciencias Exactas, Pinto 399, 7000 Tandil, Argentina

and

J. G. Reyna Almandos and M. Gallardo

Centro de Investigaciones Ópticas, Casilla de Correo 124, 1900 La Plata, Argentina

Received September 15, 1987; accepted November 12, 1987

Abstract

The spectrum of doubly ionized xenon has been investigated. The study is based on photographic recordings of xenon spectra in the 490–8900 Å range. The number of classified lines has been increased from about 300 to about 1400. The lines have been classified as transitions between 73 even levels belonging to the $5s^2 5p^4$, $5s^2 5p^3 6p$, $4f$, $5f$ and $5s^0 5p^6$ configurations, and 83 odd levels belonging to the $5s 5p^3$, $5s^2 5p^1 6s$, $7s$, $5d$ and $6d$ configurations. In particular, the classifications include most of the Xe III laser lines. The experimentally observed level structures are compared with the results of Hartree–Fock calculations and least-squares fits. A comparison is also made between the results of the present analysis and the published data on the Xe N_{4.5}OO Auger spectrum.

1. Introduction

The doubly ionized xenon atom, Xe²⁺ ($Z = 54$), is isoelectronic with neutral tellurium. The ground configuration in this sequence is $5s^2 5p^4$. Although there has been a great demand, e.g., from laser and collision physics, for improved data on the Xe III spectrum and energy level system for many years, very little work has been reported since the 1930's when Boyce [1], Humphreys [2] and Humphreys *et al.* [3] undertook extensive studies of the spectrum. A few reports have appeared treating the lower levels of the spectrum [4–6] and the $5s^0 5p^6 1S_0$ level [7, 8].

A large number of strong xenon laser lines were reported some 20 years ago [9]. Primarily due to the work of the group in La Plata, the laser lines were classified as originating in doubly and trebly ionized xenon, but no further classifications were possible due to the lack of relevant spectroscopic data.

In the present investigation we have recorded xenon spectra photographically in the 490–6900 Å range. When analysing the vast amount of experimental data we have made extensive use of Hartree–Fock calculations and parametric fits. Configuration-interaction (CI) effects, including Rydberg series CI, have been included in the calculations. The configurations studied are $5s^2 5p^4$, $5s 5p^3$, $5s^0 5p^6$, $5s^2 5p^1 6p$, $6s$, $7s$, $5d$, $6d$ and $4f$. The lowest term of the $5f$ configuration has also been located. The number of classified lines has been increased from about 300 to, in all, 1400. These lines originate from transitions between 73 even- and 83 odd-parity levels. As a consequence of the present analysis it has been possible to classify the majority of the laser lines ascribed to Xe III.

The extended analysis of the Xe III spectrum also has

some consequences for the interpretation of the Auger spectrum following ionization in the $4d$ subshell of neutral xenon.

2. Experimental

The vacuum-ultraviolet part of the spectrum was recorded in Lund. Two different light sources were used: a direct-current hollow-cathode discharge [10] and a theta-pinch discharge [11]. The hollow-cathode source gives a Xe III spectrum of better quality as regards resolution and obtainable wavelength accuracy, while the theta-pinch exposures were of great value in the determination of the ionization stages of the observed lines. The spectrum was photographed on a 3 m normal-incidence spectrograph with a plate factor of 2.77 Å/mm in the first diffraction order [12]. The wavelength range above 2000 Å was recorded on a 3.4 m Ebert plane-grating spectrograph in La Plata. This instrument has a plate factor of 5 Å/mm in the first diffraction order. The results of the wavelength measurements in air have been discussed previously [13]. The spectrum was excited in a laser-tube-like source (without end-mirrors) about 1 m in length and with an inner diameter of 3 mm. The tube has inner electrodes and was viewed end-on [14].

The wavelengths and intensities of all classified Xe III lines are given in Table I. In the long-wavelength end of the spectrum, outside the range covered by the present recording, a few lines have been included from an unpublished xenon line-list by Humphreys [15]. The quality of the recorded spectra does not permit very accurate wavelength determination. Most lines are fairly wide. The overall wavelength accuracy is estimated to be 0.05 Å in the air region and 0.02 Å in the vacuum-ultraviolet wavelength region.

The intensity figures are visual estimates of photographic density, and are on a uniform scale only within limited wavelength ranges. For the lines quoted from Humphreys' list the intensities are on a completely different scale.

All the experimentally established Xe III levels are given in Tables II and III. The level values were determined by a least-squares procedure in which the appropriately weighted wave numbers of the identified lines were used as input. All level designations are in LS notation. In most cases the names given to the levels were taken from least-squares fits of the theoretical energy expressions to the experimentally observed level values. In general, the calculated purities of the states

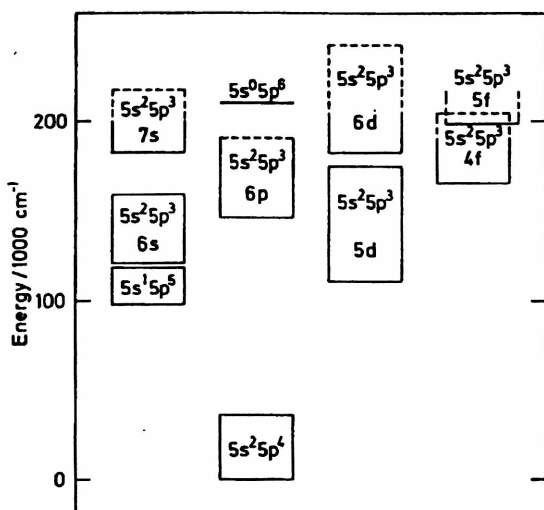


Fig. 1. Gross structure of the observed Xe III configurations. Broken lines indicate that not all levels of the configuration have been located.

(Tables II and III) are low, showing that the coupling conditions in the configurations investigated are intermediate.

3. Analysis

When performing the analysis of the experimental data we were guided by theoretical predictions of the level structures. Such predictions were obtained by diagonalization of the appropriate energy matrices, including CI matrix elements. The radial parts of the matrix elements were determined in Hartree-Fock calculations. Approximate scaling factors were determined from comparisons with calculations for similar structures. Figure 1 shows the relative positions and extensions of the configurations studied. The levels in $5s^25p^4$, $5s5p^5$ and $5s^05p^6$ were known from earlier investigations, though the designation of one level, $5s5p^5\ ^1P_1$, has been revised. The $5s^25p^3nl$ configurations can be considered as being built on the ground configuration of Xe IV, $5s^25p^3$, with the addition of an outer electron. The parent configuration gives three terms, namely 4S , 2D and 2P . Almost all levels of the $5s^25p^36p$, $6s$ and $5d$ configurations have been experimentally established or verified in this work. In the $4f$ configuration, five of the levels based on the 2P parent term are missing and in the $5s^25p^37s$ and $6d$ configurations only levels based on the 4S and 2D parent terms have been located. In the $5f$ configuration, only the levels belonging to the lowest term, (4S) 5F , have been located with certainty.

Figure 1 shows that there is severe overlapping of configurations of the same parity. This leads to heavy mixing of states belonging to different configurations, even if the matrix elements connecting the states are small. Such mixing occurs between $6s$ and $5d$, $7s$ and $6d$ and between $6p$ and $4f$ states.

3.1. Even configurations

When interpreting the observed energy-level structure of the even-parity configurations, the total energy matrix for the $5s^25p^4 + 5s^25p^3(6p + 4f + 5f) + 5s5p^45d + 5s^05p^6$ configurations was diagonalized. The calculated energy-level values were fitted to the observed ones by least-squares fits in which some of the energy parameters were treated as free parameters (Tables IV and V).

As is evident from Fig. 1, there are large energy separations between the levels of the ground configuration and the excited configurations. In cases like this, it is customary to diagonalize the energy matrix and to perform a least-squares fit for the ground configuration separately. However, it was found that a least-squares fit to the levels of the ground configuration, omitting the effective configuration-interaction parameter α , gives a large discrepancy between the observed and the calculated positions of the $5s^25p^4\ ^1D_2$ level. The radial integral in the CI matrix element between the s^2p^4 and s^0p^6 configurations is very large ($\sim 67000 \text{ cm}^{-1}$). A simple perturbation calculation indicates that this interaction gives rise to a large shift ($\sim 8000 \text{ cm}^{-1}$) of the 1S_0 level of the ground configuration. In a similar way, it was found that the interaction between the ground configuration and a "pure" $5s5p^45d$ configuration gives rise to large shifts ($\sim 4000 \text{ cm}^{-1}$) of the 3P and 1D levels, but not to the 1S_0 level. Evidently, large specific level shifts may occur from these interactions between distant configurations. It was also found that the $5s^05p^6\ ^1S_0$ state interacts strongly with the 1S_0 state of the $5s5p^45d$ configuration and a substantial mixing of these two states occurs.

In the light of the above discussion we decided to include the ground configuration and the high-lying $5s5p^45d$ configuration in the energy matrix of the even configurations. CI effects between all the configurations were taken into account. In particular, it was found that the large specific deviation of the $p^4\ ^1D_2$ level was removed in this way, even with the configuration interaction parameters fixed at their HF values. As none of the levels belonging to the $5s5p^45d$ configuration has been established experimentally, the energy parameters of this configuration were held fixed at their HF values during the fitting process (except the $F^2(5p, 5p)$ integral which was scaled to 0.8 times the HF value.)

The level structure of the $5s^25p^36p$ and $4f$ configurations is given in Fig. 2. The positions of the observed levels of the lowest term of the $5f$ configuration are also indicated. It turns out that $4f$ is almost as low a configuration as $6p$. This reflects the fact that Xe III is close to the lanthanides and $4f$ is no longer hydrogenic. All levels are given in LS notation. Generally the designations given represent the largest contribution to the eigenvector. However, for many levels the purities are very low, the largest component amounting to only about 30% in some cases. In one case we have used the second largest eigenvector component to name the level. Thus the LS designations often have very little physical significance.

3.2. Odd configurations

The odd-parity configurations were also interpreted by means of energy matrix diagonalizations and parametric least-squares fits to the energy levels. The energy matrix included the $5s5p^5 + 5s^25p^3(6s + 7s + 5d + 6d)$ configurations (Tables VI and VII).

The detailed structure of the $5s5p^5$ and the $5s^25p^3(5d + 6s)$ configurations is shown in Fig. 3. The experimentally established part of the $5s^25p^3(6d + 7s)$ configurations is shown in Fig. 4. As can be seen from the figures, there are a number of fortuitous coincidences between $6s$ and $5d$ levels, and between $7s$ and $6d$ levels causing severe mixing of the corresponding states.

All levels are given in LS notation, but, as for the even-parity levels, the designations often have very little physical significance because of the severe mixing of states with

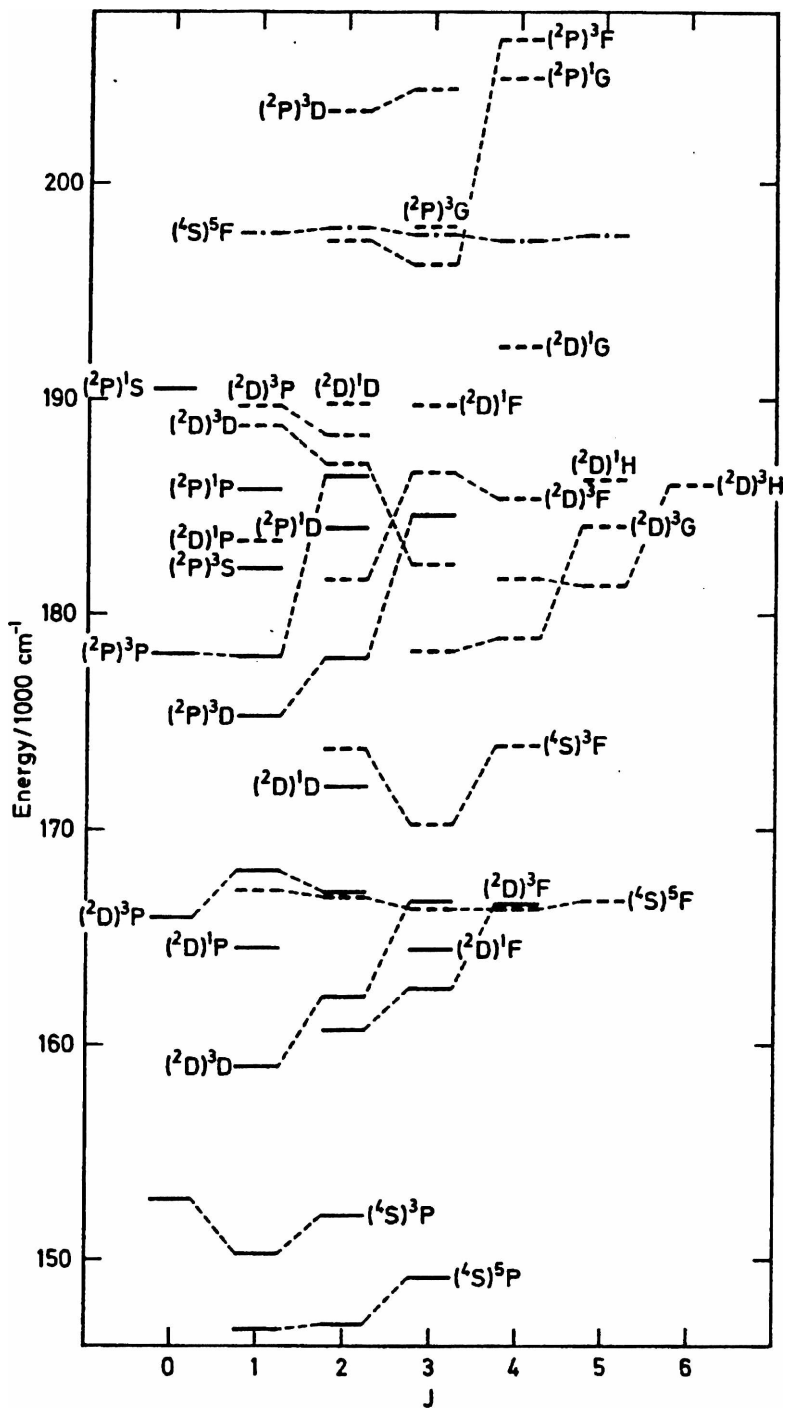


Fig. 2. Structure of the $5s^2 5p^3 (6p + 4f)$ configurations of Xe III. The position of the lowest $5f$ term is also indicated. $6p$ levels are indicated by fully

drawn lines, $4f$ levels by dashed and $5f$ levels by broken lines with dots in the centre. All levels are given in the LS coupling scheme.

different L and S values. To avoid duplication of labels it has sometimes been necessary to use the second largest or even the third largest eigenvector component to name the level.

There is also strong mixing between $5s5p^5$ and $5s^2 5p^3 5d$ states. Primarily this mixing is not caused by close level coincidences, but rather by large matrix elements connecting the states. The mixing is most pronounced for the singlets. In fact, there is no level having $5s5p^5 1P$ as its largest eigenvector component. On the other hand, there are five levels having a substantial $5s5p^5 1P$ contribution to their eigenvectors. As will be discussed below, this mixing has some consequences

for the Auger spectrum following ionization of an inner $4d$ electron.

A general observation regarding $p^3 d$ configurations seems to be that the 3S term of the lowest d configuration is predicted far below its observed position. In the $4p^3 4d$ configuration of Kr III [16], Rb IV [17], Sr V [18], and Y VI [19] the discrepancy is of the order of 3000 cm^{-1} . The discrepancy is also present in lighter elements, for instance in the $2p^3 3d$ configuration of Ne III [20]. It was shown in Refs [17] and [18] that, to a large extent, the discrepancy in the $4p^3 4d$ configurations of Sr V and Rb IV could be accounted for by the introduction of Rydberg-series configuration interactions, in

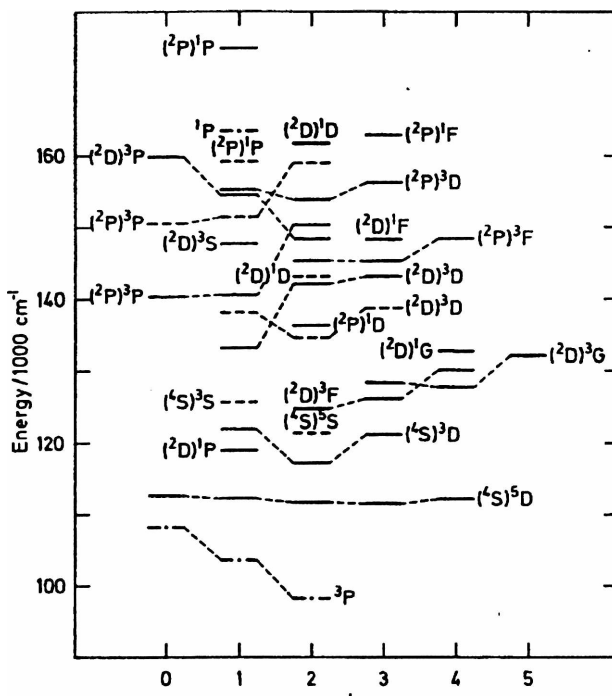


Fig. 3. Structure of the $5s5p^5 + 5s^2 5p^3 (5d + 6s)$ configurations of Xe III. $5p^5$ levels are indicated by broken lines with dots in the centre, $6s$ levels by dashed and $5d$ by fully drawn lines. All levels are given in the LS coupling scheme.

particular the $4d \leftrightarrow 5d$ interaction, in the theoretical predictions of the level structure.

In Xe III the deviation between the observed and the calculated positions of the $5p^3 5d$ 3S_1 level is 700 cm^{-1} , even when using fitted values of the energy parameters. When introducing the Rydbergseries configuration interaction the

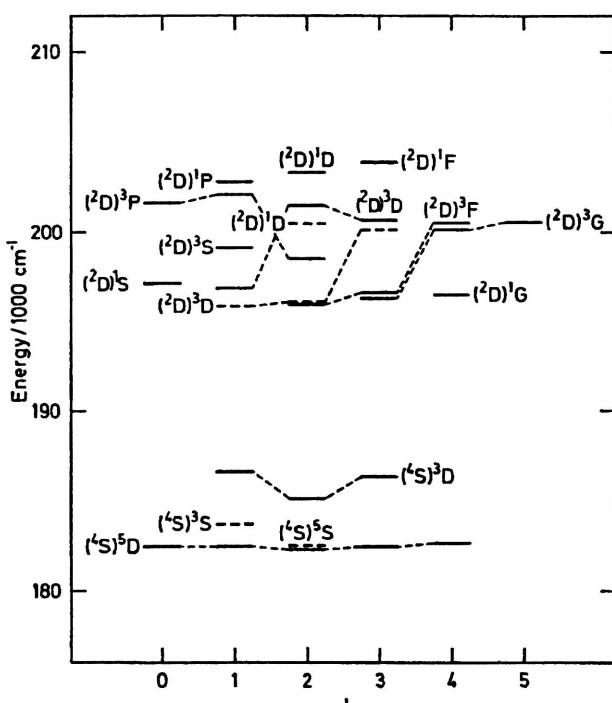


Fig. 4. Structure of the $5s^2 5p^3 (6d + 7s)$ configurations of Xe III. Only levels based on the 4S and 3D parent terms are experimentally established and indicated in the figure. $6d$ levels are indicated by fully drawn lines and $7s$ levels by dashed lines. All levels are given in the LS coupling scheme.

deviation decreases to 170 cm^{-1} . At the same time the overall mean error of the fit decreases by approximately 20%. The $5d \leftrightarrow 6d$ R^3 CI integral could not be treated as an adjustable parameter at the same time as the R^1 and R^2 CI integrals. The R^3 integral was therefore optimized in a series of separate calculations and kept fixed in the final calculation.

In general there is good agreement between the g_J factors determined in the least-square fit and those obtained experimentally by Humphreys *et al.* [3] (Table VI). We have no reasonable explanation for the small observed g_J factors of the two $J = 1$ levels at $133\,234$ and $138\,145\text{ cm}^{-1}$.

4. Discussion

Recently, much effort has been devoted to the construction of VUV lasers. One recently observed [21] VUV laser transition is the transition at 1089 \AA in Xe^{2+} connecting the odd level at $119\,026\text{ cm}^{-1}$ above the ground state, and the even-parity $5s^0 5p^6 ^1S_0$ state at $210\,857\text{ cm}^{-1}$. The lower state, previously designated as $5s5p^5 ^1P_1$, is considered to decay rapidly to the ground state while the upper state can be populated by Auger processes.

As already pointed out, there is considerable mixing between the $5s5p^5$ and the $5s^2 5p^3 5d$ states, and in the present analysis the lower level has been designated $5s^2 5p^3 (^2D) 5d$ 1P_1 . The purity of the state is only 44% and the $5s5p^5 ^1P_1$ contribution is 28%. The $5s5p^5 ^1P_1$ state is mixed into a number of different $5d$ states and this opens many different decay modes for the upper $5s^2 5p^6 ^1S_0$ state. This fact probably has to be taken into account when discussing the possible efficiency of the laser action of this particular transition.

The present analysis, in particular as regards the mixing between the $5s5p^5$ and the $5s^2 5p^3 5d$ states, also has consequences for the interpretation of the Auger spectrum of xenon following the ionization of a $4d$ electron, the $\text{N}_{4,5}\text{OO}$ spectrum (Fig. 5). The spectrum shown was recorded by Werme *et al.* [22], but has also been extensively studied by Southworth *et al.* [23], and Aksela *et al.* [24].

The spectrum consists of lines corresponding to the Xe^{2+} ion being left in different final states. There are two lines possible for each final state, corresponding to the fine structure of the initial hole in the $4d$ shell. One group of strong lines corresponds to the ion being left in the $5s5p^4$ configuration, another group to the $5s5p^5$ final states and a third group corresponds to the ion being left with an empty $5s$ shell, i.e., the configuration $5s^0 5p^6$. The additional strong lines are satellites and are mainly caused by final-state configuration interaction, i.e., in the terminology of the present study, by the mixing between the $5s5p^5$ and the $5s^2 5p^3 5d$ (and possibly $6s$) states.

A detailed comparison between the Auger data and the present optical data is given in Table VIII. The energy of the $5s^2 5p^4 ^3P_2$ ground level is set to zero. The agreement in relative energies is very good; the deviation never exceeding the estimated uncertainties in the Auger values ($\approx 0.05\text{ eV}$). The largest discrepancy is found for the $(^2P)6s$ 1P_1 level. However, the identification of this state in the Auger spectrum is tentative as it is based on a single line. Moreover, this line is doubly classified. It can also be seen that those $5d$ levels which have a significant $5s5p^5$ contribution to the eigenvector give rise to strong satellite lines in the Auger spectrum.

The new classifications for the Xe^{2+} laser lines are sum-

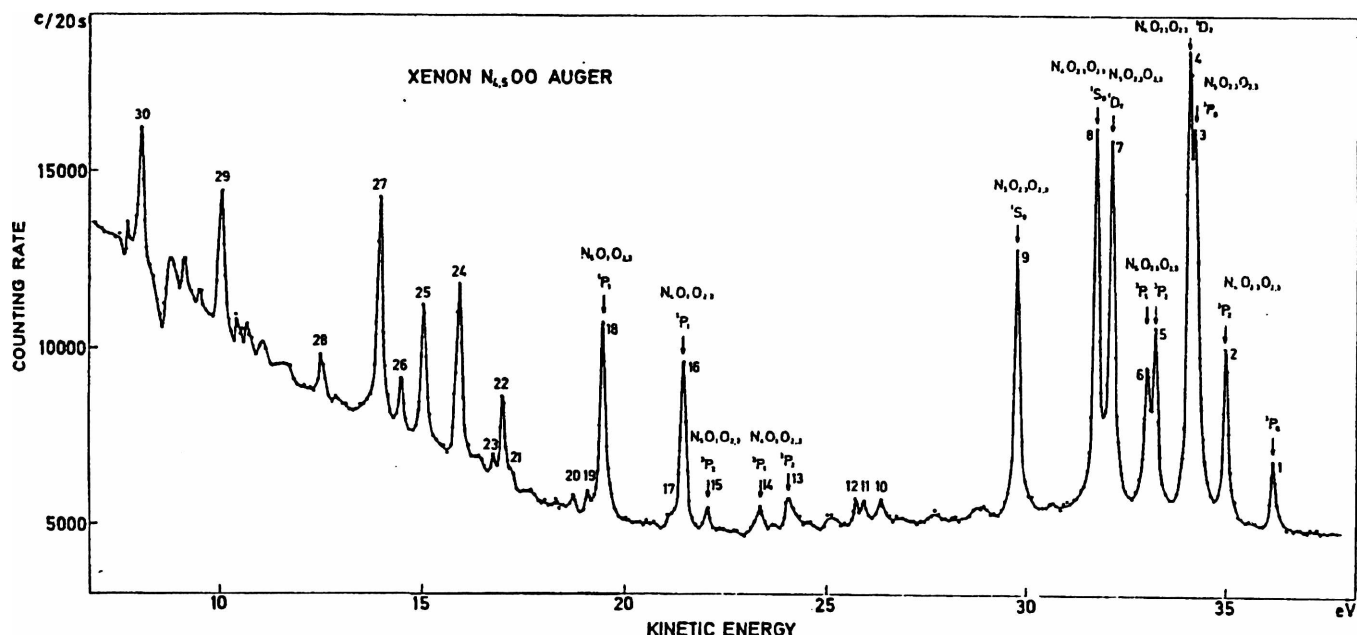


Fig. 5. Xenon $N_{4,5}OO$ Auger spectrum, from Ref. [22] (with permission from the authors).

marized in Table IX. The laser data are taken from the compilation by Beck et al. [9]. Table IX includes all laser lines ascribed with certainty or with some doubt to Xe^{2+} . Only very few lines remain unclassified. We have also included a laser line at 3349 \AA , which, with a question mark, has been ascribed to Xe^{3+} , but in the present analysis has been classified as a Xe^{2+} line.

Based on a revised analysis and isoelectronic comparisons, Gallardo et al. [5] determined the value of $250\,400 \pm 300 \text{ cm}^{-1}$ ($31.05 \pm 0.04 \text{ eV}$) for the ionization energy of Xe^{2+} . Their value, which was about 9000 cm^{-1} lower than the previously accepted value [25], is in fairly good agreement with the later value by Dutil and Marmet [26]. Using electron-impact ionization of xenon they arrived at the value of $31.24 \pm 0.10 \text{ eV}$. The present analysis does not indicate any need for revising the value of the ionization energy.

Acknowledgements

We are grateful for the financial support of the Consejo Nacional de Investigaciones Científicas y Técnicas, Argentina and the Swedish Natural Science Research Council.

References

- Boyce, J. C., Phys. Rev. **49**, 730 (1936).
- Humphreys, C. J., J. Res. Natl. Bur. Stand. **16**, 639 (1936).
- Humphreys, C. J., Meggers, W. F. and deBruin, T. L., J. Res. Natl. Bur. Stand. **23**, 683 (1939).
- Edlén, B., Phys. Rev. **65**, 248 (1944).
- Gallardo, M., Massone, C. A., Tagliaferri, A. A., Garavaglia, M. and Persson, W., Physica Scripta **19**, 538 (1979).
- Hansen, J. E. and Persson, W., Physica Scripta **25**, 487 (1982).
- Hertz, H., Z. Phys. **A274**, 289 (1975).
- Hansen, J. E., Meijer, F. G., Outred, M., Persson, W. and Di Rocco, H. O., Physica Scripta **27**, 254 (1983).
- Beck, R., Englisch, W. and Gürs, K., Table of Laser Lines in Gases and Vapors, p. 7, Springer-Verlag Berlin, Heidelberg, New York (1978).
- Persson, W. and Minnhagen, L., Ark. Fys. **37**, 273 (1968).
- Pettersson, S.-G., Physica Scripta **26**, 296 (1982).
- Minnhagen, L., Physica Scripta **11**, 38 (1975).
- Gallardo, M. and Reyna Almandos, J. G., Xenon Lines in the Range from 2000 \AA to 7000 \AA , Serie "Monografías Científicas" No. 1, Centro de Investigaciones Ópticas, La Plata (1981).
- Reyna Almandos, J. G., Gallardo, M. and Garavaglia, M., Opt. Pura Appl. **15**, 1 (1982).
- Humphreys, C. J., Unpublished.
- Persson, W., Unpublished.
- Persson, W. and Wahlström, C.-G., Physica Scripta **31**, 487 (1985).
- Persson, W. and Wahlström, C.-G., Physica Scripta **30**, 169 (1984).
- Persson, W. and Reader, J., J. Opt. Soc. Am. **B3**, 959 (1986).
- Persson, W. and Di Rocco, H. O., Work in progress; Hansen, J. E., Judd, B. R., Lister, G. M. S. and Persson, W., J. Phys. B: At. Mol. Phys. **18**, L275 (1985).
- Kapteyn, H. C., Lee, R. W. and Falcone, R. W., Phys. Rev. Lett. **57**, 2939 (1986).
- Wermel, L. O., Bergmark, T. and Siegbahn, K., Physica Scripta **6**, 141 (1972).
- Southworth, S., Becker, U., Truesdale, C. M., Kobrin, P. H., Lindle, D. W., Owaki, S. and Shirley, D. A., Phys. Rev. **A28**, 261 (1983).
- Aksela, H., Aksela, S. and Pulkkinen, H., Phys. Rev. **A30**, 865 (1984).
- Moore, C. E., Ionization Potentials and Ionization Limits Derived from the Analyses of Optical Spectra, Nat. Stand. Ref. Data Ser., Natl. Bur. Stand. NSRDS-NBS 34, Washington (1970).
- Dutil, R. and Marmet, P., Int. J. Mass. Spectrom. & Ion Phys. **35**, 371 (1980).
- Reyna Almandos, J. G., Bredice, F., Di Rocco, H. and Gallardo, M., Opt. Pura Appl. **18**, 87 (1985).

Table II. Even levels of Xe III. All levels are given in LS notation. The numbers in parentheses indicate the purities (in %) of the states

Designation	E (cm^{-1})
$5s^2 5p^4 \ ^3P_2$	0.00 (86)
3P_1	9 794.36 (98)
3P_0	8 130.08 (79)
1D_2	17 098.73 (86)
1S_0	36 102.94 (78)
$5s^2 5p^3 (^4S) 6p$	149 061.57 (84)
5P_3	146 962.42 (66)
5P_2	146 781.48 (73)
3P_2	152 057.72 (64)
3P_1	150 301.10 (57)
3P_0	152 808.17 (89)
$(^2D) 6p$	166 554.82 (82)
3F_4	162 594.81 (56)
3F_3	160 691.30 (54)
3D_3	166 699.11 (66)
3D_2	162 259.97 (47)
3D_1	158 996.98 (38)
3P_2	167 066.32 (55)
3P_1	168 086.00 (62)
3P_0	165 941.69 (84)
1F_3	164 438.64 (49)
1D_2	171 989.82 (70)
1P_1	164 511.65 (41)
$(^2P) 6p$	184 594.45 (57)
3D_3	177 955.93 (59)
3D_2	175 231.15 (66)
3P_2	186 320.88 (27)
3P_1	178 029.33 (59)
3P_0	178 054.53 (83)
3S_1	182 134.14 (58)
1D_2	184 009.10 (44)
1P_1	185 888.03 (37)
1S_0	190 491.16 (67)
$5s^2 5p^3 (^4S) 4f$	166 743.80 (84)
5F_5	166 355.27 (64)
5F_4	166 374.06 (74)

Table II. Continued

Designation	E (cm^{-1})
5F_2	166 880.09 (81)
5F_1	167 173.54 (87)
3F_4	173 946.53 (65)
3F_3	170 250.15 (42)
3F_2	173 734.12 (77)
$(^2D) 4f$	186 086.52 (100)
3H_6	181 356.80 (36)
3H_5	181 684.94 (56)
3H_4	184 114.53 (81)
3G_5	178 887.17 (58)
3G_4	178 306.08 (51)
3F_4	185 406.74 (42)
3F_3	186 614.26 (67)
3F_2	181 593.70 (41)
3D_3	182 377.01 (42)
3D_2	186 992.43 (25)
3D_1	188 792.52 (92)
3P_2	188 412.56 (38)
3P_1	189 701.46 (79)
3P_0	183 472.95 (70)
$(^2P) 4f$	197 953.29 (29)
3G_3	206 760.00 (30)
3F_4	196 156.21 (51)
3F_3	197 254.25 (43)
3F_2	204 382.87 (43)
3D_3	203 359.91 (51)
3D_2	204 904.40 (34)
3D_1	197 460.67 (89)
3P_3	197 310.57 (74)
3P_2	197 585.82 (56)
3P_1	197 860.38 (68)
3P_0	197 611.00 (90)
$5s^0 5p^6 \ ^1S_0$	210 857.49 (56)

Table III. Odd levels of Xe III. All levels are given in LS notation. The numbers in parentheses indicate the purities (in %) of the states

Designation	E (cm^{-1})
$5s5p^3 \ ^3P_2$	98 262.47 (75)
3P_1	103 568.20 (62)
3P_0	108 333.76 (55)
1P_1	163 527.40 (27)
$n = 6$	$n = 7$
$5s^2 5p^1 (^4S) ns$	121 475.94 (87)
3S_1	125 617.06 (78)
$(^2D) ns$	138 658.20 (83)
3D_3	134 667.42 (33)
2D_2	138 145.49 (49)
3D_1	143 048.20 (54)
$(^2P) ns$	158 928.10 (53)
3P_2	151 482.43 (46)
3P_1	150 505.31 (87)
1P_1	159 388.18 (32)
$n = 5$	$n = 6$
$5s^2 5p^1 (^4S) nd$	112 271.78 (88)
5D_4	111 605.41 (80)
5D_3	111 856.38 (78)
5D_2	112 449.90 (87)
5D_1	112 693.95 (69)
3D_3	121 229.58 (37)
3D_2	117 240.08 (27)
3D_1	121 922.75 (51)
$(^2D) nd$	132 159.94 (100)
3G_5	127 782.14 (40)
3G_4	128 349.15 (66)

Table III. Continued

Designation	E (cm^{-1})
1G_4	132 711.78 (73)
3F_4	130 173.73 (71)
3F_3	126 119.77 (58)
3F_2	124 691.33 (52)
1F_3	148 412.84 (42)
3D_3	143 156.24 (38)
3D_2	142 064.27 (24)
3D_1	133 234.01 (36)
1D_2	161 809.98 (39)
3P_2	148 370.13 (39)
1P_1	154 639.37 (20)
3P_0	160 733.77 (43)
1P_1	119 026.03 (44)
3S_1	147 797.41 (49)
1S_0	197 090.86 (58)
$(^2P) nd$	148 535.52 (70)
3F_4	145 340.91 (56)
3F_3	145 300.13 (50)
1F_3	162 957.50 (40)
3D_3	156 392.68 (33)
3D_2	153 893.20 (28)
3D_1	155 400.90 (45)
1D_2	136 367.48 (15)
3P_2	150 404.24 (54)
3P_1	140 730.93 (44)
3P_0	140 437.79 (42)
1P_1	175 052.36 (64)

Table IV. *Continued*

<i>J</i>	<i>E(obs)</i>	<i>E(calc)</i>	<i>obs - calc</i>	<i>g_J(obs)</i>	<i>g_J(calc)</i>	Percentage composition
	183 473	183 352	121	0.91		70 (² D)4f ¹ P + 12 (² P)4f ³ D
	185 888	186 233	-345	0.99		37 (² P)6p ¹ P + 15 (² P)6p ³ P + 14 (² D)6p ³ D + 8 (² P)6p ³ D
	188 793	188 447	345	0.54		92 (² D)4f ³ D
	189 701	190 482	-780	1.37		79 (² D)4f ³ P + 10 (² D)4f ¹ P + 5 (² P)4f ³ D
	197 611	197 587	24	0.05		90 (⁴ S)5f ⁵ F + 7 (² P)5f ³ D
0	8 130	8 271	-141			79 p ⁴ ³ P + 19 p ⁴ ¹ S
	36 103	36 012	91			78 p ⁴ ¹ S + 19 p ⁴ ³ P
	152 808	152 577	231			89 (⁴ S)6p ³ P + 6 (² P)6p ³ P
	165 942	166 239	-297			84 (² D)6p ³ P + 13 (² P)6p ¹ S
	178 055	177 654	400			83 (² P)6p ³ P + 13 (² P)6p ¹ S
	190 491	190 484	7			67 (² P)6p ¹ S + 15 (² D)6p ³ P + 7 (⁴ S)6p ³ P + 6 (² P)6p ³ P + 5 (² D)4f ³ P
		191 529				91 (² D)4f ³ P
	210 857	210 861	-3			56 p ⁶ ¹ S + 39 (¹ D)5d ¹ S

* No levels of 5s5p⁴5d have been established experimentally but the configuration is included in the theoretical treatment of the even configurations (see Section 3.1).

Table V. Energy parameters (in cm^{-1}) for the $5s^2 5p^4 + 5s^2 5p^3(6p + 4f + 5f) + 5s^0 5p^6 + 5s 5p^4 5d$ configurations of Xe III. Mean error of the least-squares fit $\sigma = [\sum(E_{\text{obs}} - E_{\text{calc}})^2 / (N - P)]^{1/2} = 331 \text{ cm}^{-1}$ with $N = 73$ known levels and $P = 22$ adjustable parameters

Parameter	HF(E_{av})	Fitted	Fitted/HF
<i>5s²5p⁴</i>			
<i>E_{av}</i>			
$F^2(5p, 5p)$	50 596	$43\ 681 \pm 1300$	0.863 ± 0.026
ζ_{sp}	6 626	7995 ± 300	1.207 ± 0.045
<i>5s²5p³6p</i>			
<i>E_{av}</i>			
$F^2(5p, 5p)$	52 840	$39\ 889 \pm 630$	0.755 ± 0.012
$F^2(5p, 6p)$	12 549	$11\ 964 \pm 760$	0.953 ± 0.061
$G^0(5p, 6p)$	2 072	$2\ 007 \pm 80$	0.969 ± 0.039
$G^2(5p, 6p)$	2 982	$2\ 443 \pm 600$	0.819 ± 0.200
ζ_{sp}	7 301	$8\ 688 \pm 150$	1.190 ± 0.021
ζ_{sp}	939	$1\ 526 \pm 120$	1.625 ± 0.130
<i>5s²5p³4f</i>			
<i>E_{av}</i>			
$F^2(5p, 5p)$	51 553	$38\ 033 \pm 720$	0.738 ± 0.014
$F^2(5p, 4f)$	29 252	$24\ 040 \pm 900$	0.822 ± 0.031
$G^2(5p, 4f)$	22 845	$18\ 859 \pm 720$	0.825 ± 0.032
$G^4(5p, 4f)$	15 446	$9\ 950 \pm 920$	0.644 ± 0.060
ζ_{sp}	6 920	$8\ 421 \pm 190$	1.217 ± 0.027
ζ_{sp}	48	0 ± 60	0.000 ± 1.250
<i>5s²5p³5f</i>			
<i>E_{av}</i>			
$F^2(5p, 5p)$	52 207	$41\ 766 \text{ (fix)}$	0.800
$F^2(5p, 5f)$	12 582	$12\ 582 \text{ (fix)}$	1.0
$G^2(5p, 5f)$	8 811	$8\ 811 \text{ (fix)}$	1.0
$G^4(5p, 5f)$	6 274	$6\ 274 \text{ (fix)}$	1.0
ζ_{sp}	7 102	$7\ 102 \text{ (fix)}$	1.0
ζ_{sp}	33	33 (fix)	1.0
<i>p⁶</i>			
<i>E_{av}</i>			
		$251\ 540 \pm 590$	
<i>5s5p⁴5d</i>			
<i>E_{av}</i>			
$F^2(5p, 5p)$	51 463	$41\ 170 \text{ (fix)}$	0.800
$F^2(5p, 5d)$	36 501	$36\ 501 \text{ (fix)}$	1.0
$G^1(5s, 5p)$	68 320	$68\ 320 \text{ (fix)}$	1.0
$G^1(5s, 5d)$	26 862	$26\ 862 \text{ (fix)}$	1.0
$G^1(5p, 5d)$	41 701	$41\ 701 \text{ (fix)}$	1.0

Table V. Continued

Parameter	HF(E_{av})	Fitted	Fitted/HF
$G^3(5p, 5d)$	25 951	25 951 (fix)	1.0
ζ_{sp}	6 893	6 893 (fix)	1.0
ζ_{sd}	381	381 (fix)	1.0
Configuration interaction integrals			
p^4-6p			
$R^2(5p5p, 5p6p)$	5419 (349)*	5419 (fix)	1.0
p^4-4f			
$R^2(5p5p, 5p4f)$	-32 918 (-.940)	-32 918 (fix)	1.0
p^4-5f			
$R^2(5p5p, 5p5f)$	-20 304 (-.911)	-20 304 (fix)	1.0
p^4-5d			
$R^1(5s5p, 5p5d)$	51 463 (.998)	51 463 (fix)	1.0
$R^2(5s5p, 5d5p)$	37 121 (.996)	37 121 (fix)	1.0
p^4-p^6			
$R^1(5s5s, 5p5p)$	67 375 (1.000)	67 375 (fix)	1.0
$6p-4f$			
$R^2(5p6p, 5p4f)$	3 107 (.197)	3 107 (fix)	1.0
$R^2(5p6p, 4f5p)$	-2 428 (-.220)	-2 428 (fix)	1.0
$6p-5f$			
$R^2(5p6p, 5p5f)$	-4 503 (-.530)	-4 503 (fix)	1.0
$R^2(5p6p, 5f5p)$	2 450 (-.360)	2 450 (fix)	1.0
$6p-5d$			
$R^1(5s6p, 5p5d)$	7 831 (.331)	7 831 (fix)	1.0
$R^2(5s6p, 5d5p)$	-2 443 (-.199)	-2 443 (fix)	1.0
$4f-5f$			
$R^2(5p4f, 5p5f)$	15 068 (.859)	8 670 ± 5160	0.575 ± 0.340
$R^2(5p4f, 5f5p)$	13 820 (.896)	13 159 ± 1584	0.952 ± 0.120
$R^2(5p4f, 5f5p)$	9 594 (.960)	9 594 (fix)	1.0
$4f-5d$			
$R^1(5s4f, 5p5d)$	-37 462 (-.894)	-17 636 (fix)	0.471
$R^2(5s4f, 5d5p)$	-24 234 (-.941)	-24 234 (fix)	1.0
$5f-5d$			
$R^1(5s5f, 5p5d)$	-16 823 (-.720)	-7 920 (fix)	0.471
$R^2(5s5f, 5d5p)$	-14 589 (-.910)	-14 589 (fix)	1.0
$5d-p^6$			
$R^1(5s5d, 5p5p)$	50 988 (.998)	50 988 (fix)	1.0

* The values in parentheses are a measure of the amount of cancellation which occurred in forming the integral. These numbers are the ratio of the true R^k value to an R^k value calculated using the absolute value of each wavefunction.

Table VI. Comparison between observed and calculated energy-level values (in cm^{-1}) and calculated percentage compositions for the $5s5p^5 + 5s^2 5p^3(6s + 7s + 5d + 6d)$ configurations of Xe III. Eigenvector components larger than 5% are given. Observed [3] and calculated g_j factors are listed

J	E(obs)	E(calc)	obs - calc	g _j (obs)	g _j (calc)	Percentage composition
5	132 160	132 443	-283		1.20	$100(^2D)5d^3G$
	200 472	200 436	35		1.20	$100(^2D)6d^3G$
4	112 272	112 250	21		1.47	$88(^4S)5d^5D + 10(^2P)5d^3F$
	127 782	127 735	47		1.16	$40(^2D)5d^3G + 27(^2D)5d^3F + 16(^2P)5d^3F + 9(^2D)5d^1G + 7(^4S)5d^5D$
	130 174	130 702	-528		1.20	$71(^2D)5d^3F + 22(^2D)5d^3G$
	132 712	132 800	-88		1.02	$73(^2D)5d^1G + 25(^2D)5d^1G$
	148 536	148 459	76		1.21	$70(^2P)5d^3F + 13(^2D)5d^4G + 12(^2D)5d^3G$
	182 716	182 754	-37		1.46	$85(^4S)6d^3D + 12(^2P)6d^3F$
	196 538	196 411	127		1.13	$42(^2D)6d^3G + 31(^2D)6d^1G + 15(^2P)6d^3F + 10(^4S)6d^3D$
	200 051	200 074	-24		1.06	$43(^2D)6d^6G + 42(^2D)6d^1G + 15(^2D)6d^3F$
	200 426	200 451	-25		1.21	$82(^2D)6d^3F + 16(^2D)6d^4G$
3	111 605	111 401	204		1.44	$80(^4S)5d^5D + 6(^2P)5d^3F + 6(^2P)5d^3D$
	121 230	121 363	-133		1.29	$37(^4S)5d^3D + 25(^2D)5d^3D + 15(^4S)5d^3D + 6(^2D)5d^3G + 6(^2P)5d^3F + 5(^2D)5d^3F$
	126 120	126 121	-1		1.12	$58(^2D)5d^3F + 11(^4S)5d^3D + 11(^2D)5d^3D + 10(^2P)5d^3F + 8(^2D)5d^3G$

